

# Modeling Spatial Distributions of Base Stations in Cellular Networks

Qianlan Ying\*, Zhifeng Zhao\*, Yifan Zhou\*, Rongpeng Li\*, Xuan Zhou\*, and  
Honggang Zhang\*<sup>†</sup>

\* Zhejiang University, Zheda Road 38, Hangzhou 310027, China

Email: {greenjelly, zhaozf, zhouyftt, lirongpeng, zhouxuan,  
honggangzhang}@zju.edu.cn

<sup>†</sup>Université Européenne de Bretagne (UEB) & Supélec, Avenue de la Boulaie CS  
47601, Cesson-Sévigné Cedex, France

## Abstract

The topology of base stations (BSs) in cellular networks, serving as a basis of networking performance analysis, is considered to be obviously distinctive with the traditional hexagonal grid or square lattice model, thus stimulating a fundamental rethinking. Recently, a new stochastic geometry approach based on the *Poisson point process* (PPP) attracts an ever-increasing popularity in modeling BS deployment of cellular networks due to its merits of tractability and capability for capturing non-uniformity. In this letter, we perform a detailed comparison between the PPP model and real base station locations. Our results indicate that the PPP fails to precisely characterize either urban or rural BS deployment. Furthermore, we examine the topology of urban and rural deployment separately by comparing the corresponding real data with aggregative point process models as well as repulsive point process models. This comparison verifies that the capacity-centric deployment in urban areas can be modeled by typical aggregative processes such as the *Matern cluster process*, while the coverage-centric deployment in rural areas can be modeled by representative repulsive processes such as the *Strauss hard-core process*.

## I. INTRODUCTION

The topological structure of cellular networks has been gaining tremendous complexity to fulfill exponentially increasing demand for mobile data. Nowadays practical deployment of

cellular networks, which are organically deployed to provide high capacity, are considered to be highly heterogeneous and irregular [1].

Since the architecture of heterogeneous networks plays a key role in evaluating system performance in 4G and future cellular networks, analysis of the topology is emerging as a primary task for subsequent accurate performance characterization. By far, the most common assumption widely used in analytical calculations for cellular networks is that base stations (BSs) are uniformly distributed in the covered areas. Accordingly, hexagonal grids and square lattices are pervasively utilized to model the locations of BSs. Both models, however, are generally intractable and structurally different from the real BS deployment.

Therefore, much of the researchers' focus has been shifting to more accurate BS spatial characterization, so as to capture the non-uniformity of practical deployment. In that regard, stochastic geometry has proven to be an effective means to model BS placement [2]. It is demonstrated in [3] that the *Poisson point process* (PPP), of which the points are independently and uniformly distributed in certain area, tracks the real configurations as accurately as the conventional grid model. Particularly, it is applicable in deriving tractable theoretical results for downlink performance evaluation under some assumptions. However, as population distributes unevenly and practical BSs tend to be deployed with an target (e.g., coverage-centric, capacity-centric) being strongly associated with human activities, the PPP exhibits some unrealistic characteristics. Conversely, alternative spatial patterns might yield superior modeling precision. For example, researchers have showed the fitness of the *Geyer saturation process* in modeling WiFi spots spatial pattern [4]. For cellular networks, Taylor et al. proposed to use the *Strauss process* and the *Geyer saturation process* to model macro-cellular deployment [5]. The study in [6] indicated the accuracy of Poisson cluster model in characterizing BS spatial distributions in large cities. Although there exists several works towards spatially modeling the BS locations in different scenarios, few of them has ever shed light on the comparison between the two typical geographical categories, i.e., urban and rural areas.

Motivated by the observations above, we try to find the most precise spatial distribution model, based on the collected BS data from the largest cellular network operator in China. Firstly, we select data subsets from the urban area and the rural area separately and demonstrate that the PPP model is pessimistic in modeling either point pattern. Instead, by means of summary statistics including the *G*-function and the *K*-function [7], [8], we measure the spatial dependence of

both kinds of regions. Furthermore, we test the hypotheses of different spatial models by the  $L$ -function and the coverage probability, and verify the accuracy of several stochastic models employed in urban and rural BS deployment, respectively.

The rest of the letter is organized as follows. In Section II, we begin with a brief overview of representative stochastic spatial models and present a description of the dataset. Then, the methodology of fitting point processes to the collected practical data is introduced in Section III. The experimental results are shown in Section IV before concluding this letter in Section V.

## II. PRELIMINARIES

### A. Background on Point Processes

Generally, a point process  $\mathbf{x}$  is a finite collection of randomly distributed locations contained in a given bounded region  $S$ . A realization of such a point process  $\{x_1, x_2, \dots, x_{N(\mathbf{x})}\}$  can be specified by the number of points  $N(\mathbf{x})$  and the joint distribution of the points in  $\mathbf{x}$ . Point processes (e.g., pairwise interaction processes, hard-core processes and clustered processes) can be grouped into three categories, the PPP, repulsive processes and aggregative processes. A PPP  $\mathbf{x}$  defined on  $S$  with the intensity measure  $\mu$  satisfies for any bounded region  $B$  belonging to  $S$  with  $\mu(B) > 0$ ,  $N(B)$  is Poisson distributed with mean  $\mu(B)$ . They possess the property of “no interaction” between nodes [9].

By contrast, a pairwise interaction process  $\mathbf{x}$  takes inter-point interactions into consideration. Its probability density function (PDF) on a compact region satisfies

$$f(\mathbf{x}) = a \cdot \prod_{i=1}^{N(\mathbf{x})} b(x_i) \cdot \prod_{i < j} c(x_i, x_j), \quad (1)$$

where  $a$  denotes a normalizing constant, while  $b(\cdot)$  and  $c(\cdot)$  are nonnegative functions, indicating first-order trends and pairwise interactions, respectively. Usually, when the functions  $b(\cdot)$  and  $c(\cdot)$  take different forms, the pairwise interaction process could be simplified to different processes:

- **Strauss process:**  $b(\cdot) = \beta$  and  $c(u, v) = \gamma$  conditional on  $0 < \|u - v\| \leq r$ ,  $c(u, v) = 1$  otherwise. Thus, we have the density function as the form

$$f(\mathbf{x}) = a\beta^{N(\mathbf{x})}\gamma^{s(\mathbf{x})}, \quad (2)$$

in which  $s(\mathbf{x})$  denotes the number of point pairs of  $\mathbf{x}$  lie within a distance  $r$ . The *Strauss process* is effective in modeling repulsion effect between nodes, yet it proves to be non-integrable for  $\gamma > 1$  corresponding to the desired clustering.

- **Geyer saturation process:** As a generalized version of *Strauss process*, a saturation limit  $sat$  is added in the exponent of  $\gamma$ , thereby trimming the total contribution from each point's pairwise interaction to a maximum  $sat$ . The process can describe both repulsive and aggregative patterns.

Hard-core processes (e.g., the Poisson hard-core process and the Strauss hard-core process), implied by the name, introduce a hard-core distance  $h_c > 0$  into its PDF [10]. Therefore, the inter-point distances between distinct points are always greater than  $h_c$ .

On the other hand, cluster processes can precisely fit point patterns with the aggregation behavior. In this letter, we primarily focus on the *Matern cluster process* (MCP), which is a special case of the Poisson cluster process. Usually, The Poisson cluster process is formed by taking a Poisson process as parent points with daughter points scattering around. In particular, we call it the MCP if the daughter points are uniformly distributed within the ball of radius  $r$ . An MCP can be further specified by other parameters, including the intensity of the parent points  $\kappa$  and the mean number of points in each cluster  $\mu$ .

## B. Dataset Description

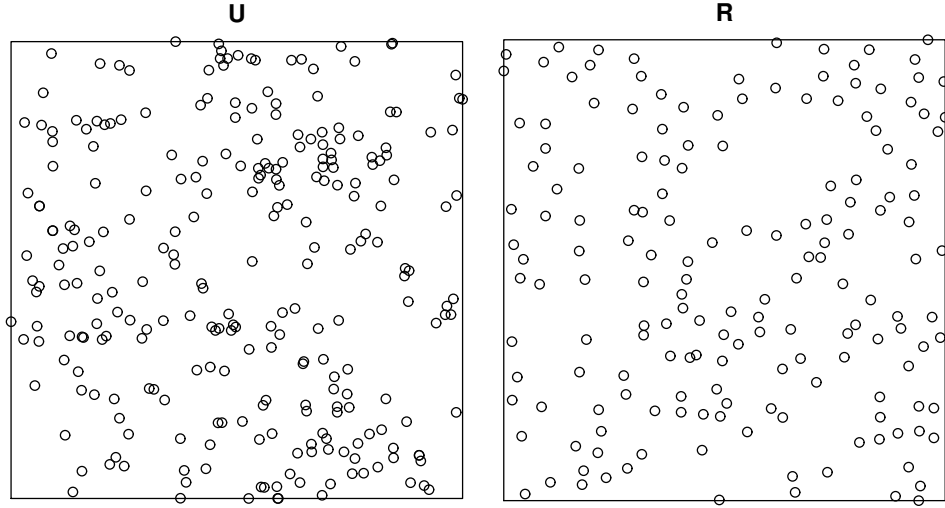


Fig. 1. (left): Distribution of the urban point pattern  $U$  with 259 BSs. (right): Distribution of the rural point pattern  $R$  with 167 BSs.

Our dataset is based on the GSM BSs within an eastern province of China. The location records of 47908 BSs are analyzed. The whole research area is divided into two typical regions,

namely the urban area and the rural area by matching the longitude and latitude information of each BS to that of the target area on a Google Map. We pick a square region  $U$  with a total space of  $7.73km^2$  from a dense urban region and a square region  $R$  covering a total area of  $1069.89km^2$  in some part of the rural area. Both regions are mapped onto unit squares as shown in Fig. 1.

### III. METHODOLOGY

This letter aims at obtaining an accurate point process to model the real BS deployment in target areas. In order to reach such a goal, this study utilizes the following fitting and analysis methods.

#### A. Fitting Method

It is common to utilize the maximum pseudolikelihood estimates as the fitting method in stochastic geometry. Whereas for models with irregular parameters such as *sat* in the *Geyer saturation process*, we can obtain the relevant parameters by analogy with the profile maximum pseudolikelihood estimator [11].

#### B. Analysis Method

The analysis of point patterns largely depends on summary statistics (e.g., the standard deviation). For testing our assumption of real data, we employ the nearest neighbor distance function (the  $G$ -function), the  $L$ -function and the coverage probability as the metrics:

1) *G-function*: The  $G$ -function is the cumulative frequency distribution of the nearest neighbor distances, which illustrates the ways the points are spaced. It indicates clustering when the  $G$ -function increases rapidly at a short distance, while it implies dispersion otherwise.

2) *L-function*: The  $L$ -function relies on the distance between the points and provides an estimate of spatial dependence over a wide range of scales. Therefore, the  $L$ -function could judge whether a pattern exhibits clustering or dispersion. Formally, the  $L$ -function is defined as  $L(r) = \sqrt{K(r)/\pi}$ . Here,  $K(r)$  is the Ripley's  $K$ -function and can be calculated as

$$K(r) = \frac{1}{\lambda} \mathbb{E}[N(\mathbf{x} \cap b(x, r) \setminus \{x\}) | x \in \mathbf{x}], \quad (3)$$

where  $\lambda$  denotes the intensity of the points [7]. If a point pattern is the PPP,  $L(r)$  would equal to  $r$ . Moreover,  $L(r) > r$  indicates clustering while  $L(r) < r$  represents dispersion.

3) *Coverage Probability*: The coverage probability is another important metric related to network performance. It indicates the probability that a randomly chosen mobile user achieves signal-to-interference ratio (SIR) larger than a threshold  $T$  [3]. Specifically, if a mobile user is connected to the BS located at point  $x_k$ , then the received downlink *SIR* has the form as:

$$SIR = \frac{Ph_k \|x_k\|^{-\alpha}}{\sum_{i: x_i \in \mathbf{x} \setminus x_k} Ph_i \|x_i\|^{-\alpha}}, \quad (4)$$

where  $P$  denotes the transmit power of each BS,  $h$  represents the multipath fading effect, and  $\alpha$  is the pass loss exponent. Here we assume all the downlink signals with equal transmit power experience Rayleigh fading and  $\alpha$  equals to 4.

#### IV. EXPERIMENTAL RESULTS AND ANALYSES

##### A. Pre-judgement

First we examine the  $G$ -function and the  $K$ -function of  $U$  and  $R$  to determine whether they are clustered or regular. The pre-judgement results will help to understand both point patterns and find appropriate spatial models.

As seen in Fig. 2, the point pattern  $U$  in dense urban area has a strong tendency of clustering between nodes with both calculation results larger than the theoretical ones (i.e., the PPP). On the contrary, the point pattern  $R$  reflects regularity as the corresponding curve in  $G$ -function increases much lower at a short distance. The result can be readily acknowledged, as coverage optimization and interference minimization contribute to spatial regularity of BS deployment. Whereas in densely populated regions, the comparatively higher amount of network traffic in urban areas contribute to intensive and clustering BS deployment.

##### B. Fitted Models

Inspired by the first-stage results above, we further examine the fitness of aggregative processes to the clustered point pattern  $U$ . The MCP and the *Geyer saturation process* are included in the fitting process. On the other hand, repulsive processes including the *Strauss hard-core process* (SH), the *Geyer saturation process* and the *Poisson hard-core process* (PHCP) are utilized to fit the more regular point pattern  $R$ . As a benchmark, the PPP is employed in both validations, which could further verify our hypotheses. Table I lists the corresponding fitting results, in

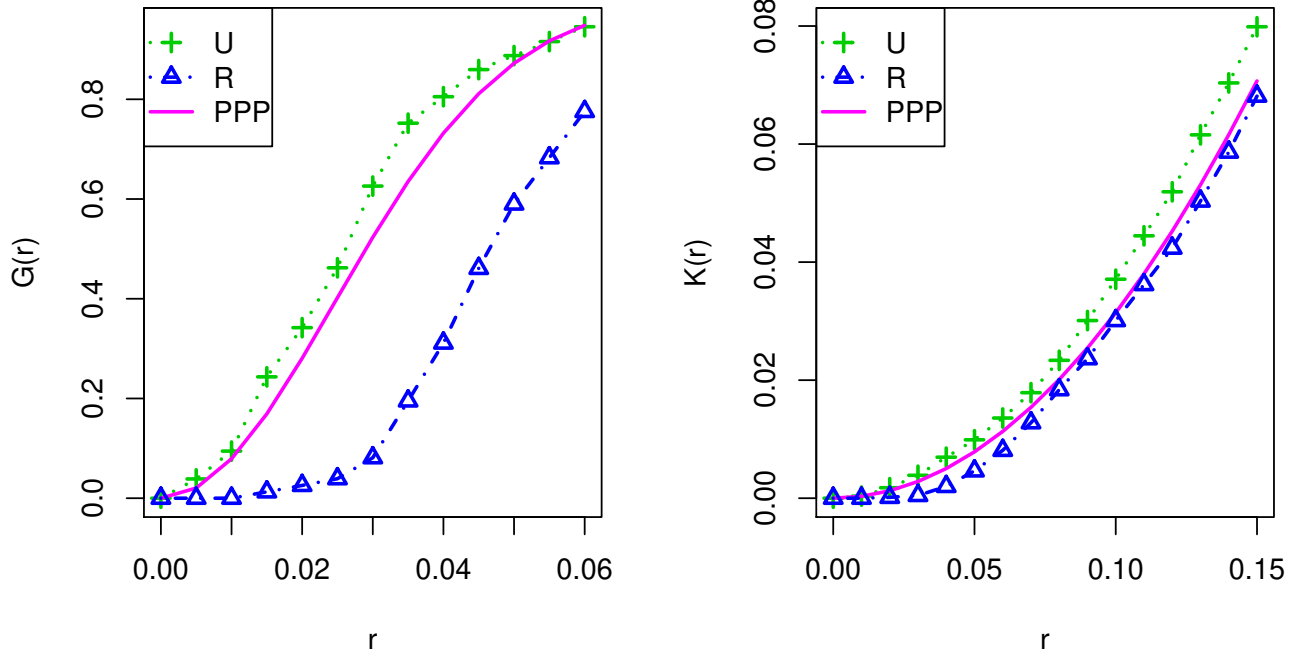


Fig. 2. (left): The  $G$ -function of  $U$ ,  $R$  and the theoretical  $G$ -function of the PPP (the solid line). (right): The Ripley's  $K$ -function of  $U$ ,  $R$  and the theoretical  $K$ -function of the PPP.

TABLE I  
PARAMETERS FOR BEST MODEL FITTING

Data type	Processes	Parameters
Urban	PPP	$\lambda = 47.50$
	Geyer	$r = 0.03$ , $sat = 4$ , $\beta = 182.93$ , $\gamma = 1.25$
	MCP	$\kappa = 162.48$ , $r = 0.067$ , $\mu = 1.61$
Rural	PPP	$\lambda = 35.75$
	PHCP	$h_c = 0.015$ , $\beta = 173.34$
	SH	$h_c = 0.015$ , $\beta = 237.24$ , $r = 0.03$
	Geyer	$r = 0.073$ , $sat = 1$ , $\beta = 26.08$ , $\gamma = 6.01$

terms of the maximum pseudolikelihood estimates and the profile maximum pseudolikelihood estimates.

We use the R package *spatstat* [8] to fit parametric models to the real data, and then generate simulated realizations using Markov Chain Monte Carlo tests.

### C. Model Validation

After the parameter estimation, the fitting accuracy of these models above are assessed based on the  $L$ -function and the coverage probability separately. For each of the fitted models, we generate 599<sup>1</sup> simulated curves and throw out 30 highest and 30 lowest values to form the pointwise envelope, which leads to a 90% confidence level. Then we judge whether the  $L$ -function and the coverage probability of the realistic point patterns lie within these confidence intervals.

The coverage probability curve is drawn under a wide range of SIR thresholds. Notably, in order to eliminate the edge effect induced by user locations, 1000 randomly selected mobile users are assumed to be located in the central part of the unit window covering  $\frac{2}{3}\text{width} \times \frac{2}{3}\text{height}$  of the total area. The coverage probability is then computed by comparing the corresponding average SIR values to the selected threshold.

1) *Urban Point Pattern*: Fig. 3 presents the fitting envelopes with the 90% confidence level of the PPP, the *Geyer saturation process* and the MCP with respect to the urban point pattern  $U$ . The  $L$ -function curves are shown in Fig. 3 (a), (c) and (e) and the coverage probability curves are plotted in the other subfigures, respectively. Obviously, we can reject the hypothesis that  $U$  is a PPP, as the observed function values on both metrics fall outside the envelope from Fig. 3 (a) and (b). According to Fig. 3 (d), we can not reject the hypothesis that  $U$  is a *Geyer Saturation process* by the coverage probability. In Fig. 3 (c), the curve of  $U$  lies outside the envelope when  $r > 0.1$ . Therefore, we can also reject the null hypothesis of the *Geyer model*. As seen in Fig. 3 (e) and (f), the MCP fits precisely to the point pattern  $U$  based on both statistics.

*Remark*: The MCP is the model that captures the properties of the urban point pattern best.

<sup>1</sup>The significance level  $\alpha$  can be calculated as  $\alpha = 2 * nrank / (1 + nsim)$ , by the number of simulations  $nsim$  and the rank of the envelope value  $nrank$ . Therefore, if we take  $nsim = 599, nrank = 30$ ,  $\alpha$  would equal 0.1.



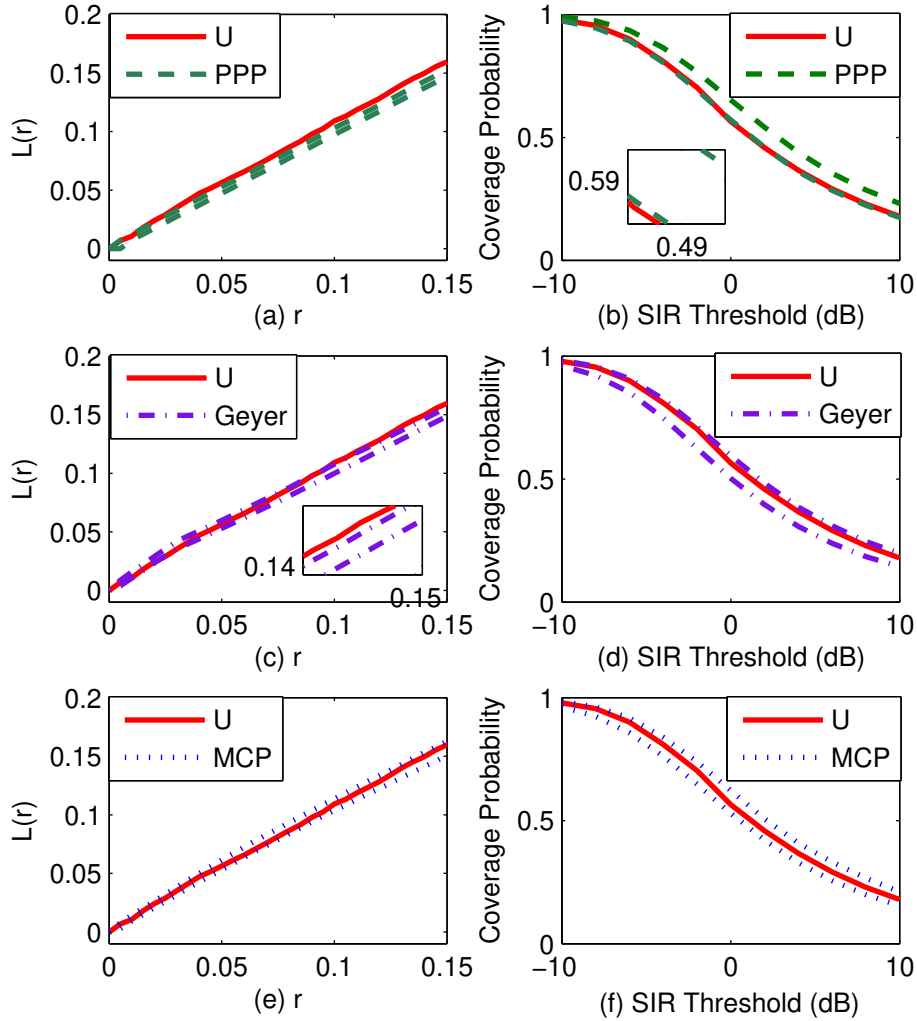


Fig. 3. (a), (c) and (e): the  $L$ -function of the point pattern  $U$  and the corresponding envelopes of fitted models; (b), (d) and (f): the coverage probability function of the point pattern  $U$  and the corresponding envelopes of fitted models.

2) *Rural Point Pattern*: Fig. 4 shows the realistic  $L$ -function and the coverage probability of the rural point pattern  $R$ , as well as the corresponding simulated envelopes, including the PPP, the PHCP, the SH and the *Geyer saturation process*. We can reject the null hypothesis of the PPP using either the  $L$ -function or the coverage probability, as seen in Fig. 4 (a) and (b), respectively. Though the PHCP and the *Geyer saturation process* satisfy the verifications based on the coverage probability, as depicted in Fig. 4 (d) and (h), we can reject these two hypotheses by Fig. 4 (c) and (g). However, we can not reject the hypothesis that  $R$  is the SH on both metrics

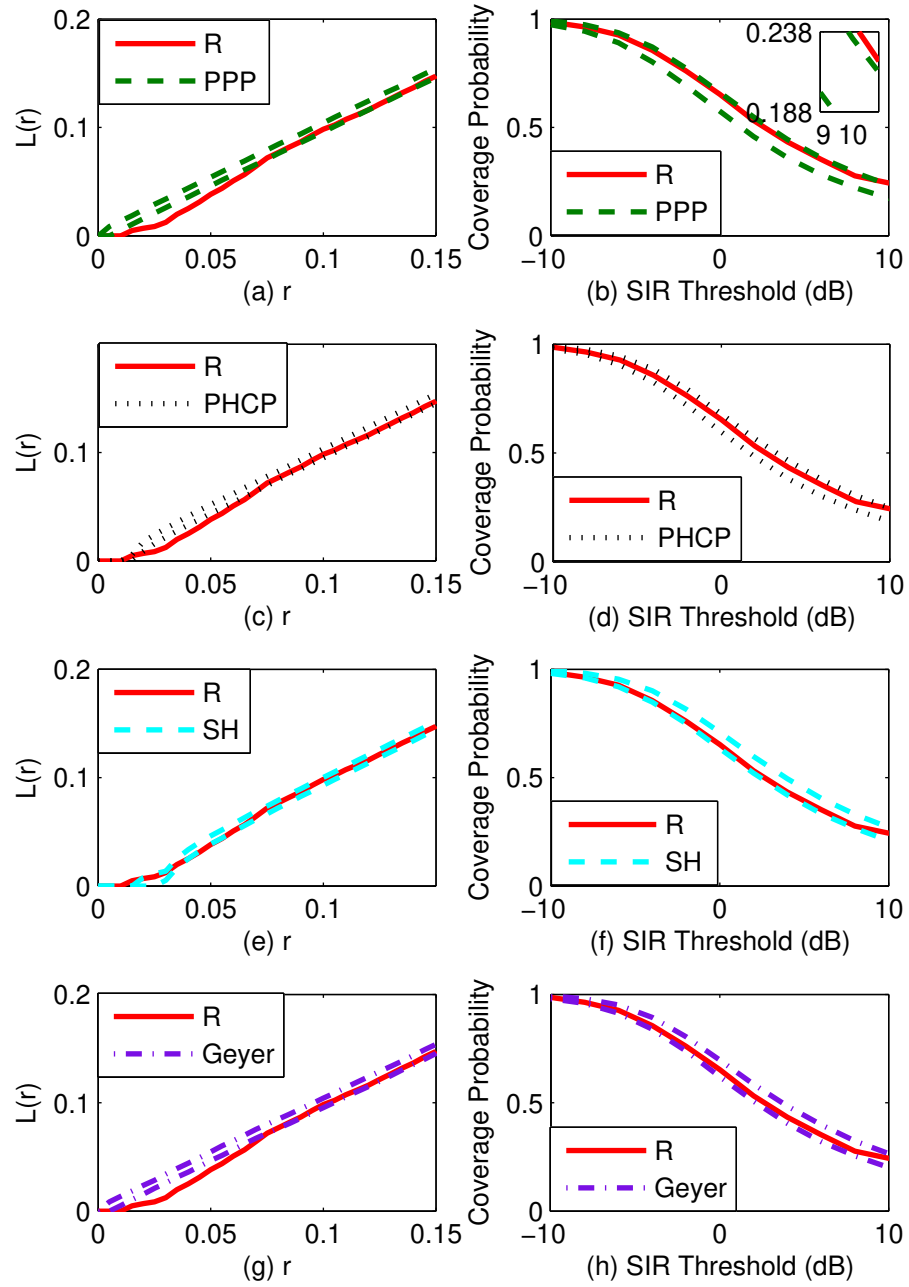


Fig. 4. (a), (c), (e) and (g): the  $L$ -function of the point pattern  $R$  and the corresponding envelopes of fitted models; (b), (d) (f) and (h): the coverage probability function of the point pattern  $R$  and the corresponding envelopes of fitted models.

according to Fig. 4 (e) and (f).

*Remark:* The SH fits best to the original rural pattern.

## V. CONCLUSION

In this letter, we studied the problem of spatially modeling BS deployments based on the data from practical deployment, and rejected the hypothesis that BS in either urban or rural area is Poisson distributed. Afterwards, the Ripley's  $K$ -function and the  $G$ -function were utilized to reveal the discrepancy between the urban and the rural BS deployment. Furthermore, we found the urban deployment expresses clustering property and could be well fitted by aggregative processes such as the *Matern cluster process*, while the rural deployment implies dispersion phenomenon and follows a *Strauss hard-core process*. The results indicate the diversity of network deployment, and thus provide effective performance analysis approach, as well as quantized reference for cellular network planning.

## ACKNOWLEDGMENT

This letter is supported by the National Basic Research Program of China (973Green, No. 2012CB316000) and the grant of "Investing for the Future" program of France ANR to the CominLabs excellence laboratory (ANR-10-LABX-07-01).

## REFERENCES

- [1] J. G. Andrews, R. K. Ganti, M. Haenggi, N. Jindal, and S. Weber, "A primer on spatial modeling and analysis in wireless networks," *IEEE Commun. Mag.*, vol. 48, no. 11, pp. 156–163, Nov. 2010.
- [2] M. Haenggi, J. G. Andrews, F. Baccelli, O. Dousse, and M. Franceschetti, "Stochastic geometry and random graphs for the analysis and design of wireless networks," *IEEE J. Sel. Area. Commun.*, vol. 27, no. 7, pp. 1029–1046, Sep. 2009.
- [3] J. G. Andrews, F. Baccelli, and R. K. Ganti, "A tractable approach to coverage and rate in cellular networks," *IEEE Trans. Commun.*, vol. 59, no. 11, pp. 3122–3134, Nov. 2011.
- [4] J. Riihijarvi and P. Mahonen, "Modeling spatial structure of wireless communication networks," in *Proc. IEEE INFOCOM Comput. Commun. Workshops*, San Diego, CA, Mar. 2010.
- [5] D. B. Taylor, H. S. Dhillon, T. D. Novlan, and J. G. Andrews, "Pairwise interaction processes for modeling cellular network topology," in *Proc. IEEE GLOBECOM*, Anaheim, CA, Dec. 2012.
- [6] C.-H. Lee, C.-Y. Shih, and Y.-S. Chen, "Stochastic geometry based models for modeling cellular networks in urban areas," *Wireless networks*, vol. 19, no. 6, pp. 1063–1072, Aug. 2013.
- [7] B. Ripley, "Modelling spatial patterns," *J. Royal Statistical Society, Series B*, vol. 39, pp. 172–212, 1977.
- [8] A. Baddeley, "Analysing spatial point patterns in R," Technical Report, CSIRO, Version 4., Tech. Rep., 2008.

- [9] J. Møller and R. P. Waagepetersen, “Modern statistics for spatial point processes,” *Scandinavian J. Stat.*, vol. 34, no. 4, pp. 643–684, Dec. 2007.
- [10] P. J. Diggle, T. Fiksel, P. Grabarnik, Y. Ogata, D. Stoyan, and M. Tanemura, “On parameter estimation for pairwise interaction point processes,” *Int. Stat. Rev.*, pp. 99–117, Apr. 1994.
- [11] A. Baddeley and R. Turner, “Practical maximum pseudolikelihood for spatial point patterns,” *Australian & New Zealand J. Stat.*, vol. 42, no. 3, pp. 283–322, Sep. 2000.